



Research on the Occurrence State of Methane Molecules in Postmature Marine shales—A Case Analysis of the Lower Silurian Longmaxi Formation Shales of the Upper Yangtze Region in Southern China

OPEN ACCESS

Edited by:

Shu Jiang,

The University of Utah, United States

Reviewed by:

Tingwei Li,

Guangzhou Marine Geological Survey,

China

Xin Li,

China National Offshore Oil

Corporation, China

Pengfei Wang,

China Geological Survey, China

*Correspondence:

Kun Zhang

shandongzhangkun@126.com

Specialty section:

This article was submitted to

Geochemistry,

a section of the journal

Frontiers in Earth Science

Received: 28 January 2022

Accepted: 07 February 2022

Published: 02 March 2022

Citation:

Zhang K, Song Y, Jiang Z, Yuan X,

Wang X, Han F, Zhang L, Tang L, Liu P,

Yang Y, Zeng Y, Chen X and Zheng Z

(2022) Research on the Occurrence

State of Methane Molecules in

Postmature Marine shales—A Case

Analysis of the Lower Silurian

Longmaxi Formation Shales of the

Upper Yangtze Region in

Southern China.

Front. Earth Sci. 10:864279.

doi: 10.3389/feart.2022.864279

Kun Zhang^{1,2,3*}, Yan Song^{4,5,6}, Zhenxue Jiang^{4,5}, Xuejiao Yuan^{1,2}, Xueying Wang^{1,2}, Fengli Han^{1,2}, Liwen Zhang^{1,2}, Liangyi Tang^{1,2}, Pei Liu^{1,2}, Yiming Yang^{1,2}, Yao Zeng^{1,2}, Xuecheng Chen^{1,2} and Zehao Zheng^{1,2}

¹School of Geoscience and Technology, Southwest Petroleum University, Chengdu, China, ²State Key Laboratory of Oil and Gas Reservoir Geology and Exploitation, Southwest Petroleum University, Chengdu, China, ³Key Laboratory of Tectonics and Petroleum Resources (China University of Geosciences), Ministry of Education, Wuhan, China, ⁴State Key Laboratory of Petroleum Resources and Prospecting, China University of Petroleum, Beijing, China, ⁵Unconventional Petroleum Research Institute, China University of Petroleum, Beijing, China, ⁶PetroChina Research Institute of Petroleum Exploration and Development, Beijing, China

The Yangtze region in southern China is endowed with abundant marine shale gas. Methane molecules exist in either adsorption state or free state in postmature marine shales, depending on the components of shales. In this study, the core samples of the selected well in the Lower Silurian Longmaxi Fm. shales from the Sichuan Basin, upper Yangtze region, southern China, were taken as study objects. We carried out TOC content, organic matter maturity, mineral component, and core gas content analyses and isothermal adsorption, FIB-SEM, and FIB-HIM experiments to analyze the occurrence state of methane molecules in postmature marine shales. The conclusions are as follows: most methane molecules exist in the organic matter pores of the postmature marine shales, and only a small amount of them exist in clay mineral pores. The organic matter pores in organic-rich shales are large in number with excellent roundness and are well connected, with large pores covering small ones. Thus, abundant free gas can be stored in the organic matter pores and pore throats, making it possible to densely and continuously adsorb methane molecules with a relatively large adsorption space. The flake-shaped clay minerals have a small number of pores with low roundness. Among the three clay minerals in postmature marine shales of the Longmaxi Fm., the I/S mixed layer offers certain reservoir spaces for adsorbed and free gases and chlorite stores a little adsorbed gas and little free gas, while illite hardly stores the adsorbed gas but contains a little free gas.

Keywords: postmature marine shales, methane molecules, free gas, adsorbed gas, organic matter pore, clay mineral pore

HIGHLIGHTS

- (1) The organic matter pores in organic-rich shales are well connected and round, presenting a structure where large pores covering small ones. The flake-shaped clay minerals have a small number of pores with low roundness.
- (2) Abundant free gas can be stored in the organic matter pores and pore throats, so the pores can continuously adsorb methane molecules with a relatively large adsorption space.
- (3) Among the three clay minerals in postmature marine shales of the Longmaxi Fm., the I/S mixed layer offers some reservoir spaces for adsorbed and free gases. Chlorite stores a little adsorbed gas and little free gas, while illite hardly stores the adsorbed gas but contains some free gas.

INTRODUCTION

In recent years, thanks to the advancement of unconventional geological theory, horizontal drilling technology, and hydraulic fracturing technology, shale gas exploration has scored a complete success in North America, changing the world energy use structure (Świąch et al., 2017). Similar to North America, China has gas-bearing basins with enormous exploration potential in shale gas resources, and the examples include the Sichuan Basin, Ordos Basin, Junggar Basin, Songliao Basin, and Bohai Bay Basin (Wei et al., 2017; Zhang et al., 2019d; Wang, 2019; Avraam et al., 2020; Wang et al., 2020a; Gao et al., 2020). The China National Petroleum Corporation and China Petrochemical Corporation have had several successful explorations in postmature marine shales in the Lower Silurian Longmaxi Fm. and its surroundings. Shale gas fields have been built in southern Sichuan, southeast Sichuan, and north Yunnan and Guizhou, with high yields of shale gas (Dong et al., 2018; Guo et al., 2019; Ma, 2019; Shang Xu et al., 2020; Xu et al., 2020). Shale gas can be divided into free gas and adsorbed gas based on the occurrence state. The former exists in the reservoir space of shales, and the latter is adsorbed onto the inner surface of the organic matter and clay minerals. Meanwhile, the adsorbed gas could transform into free gas at a specific temperature and pressure (Huang and Zhao, 2017; Chen et al., 2019; Guo et al., 2019; Kang et al., 2019; Yu et al., 2022).

Scholars have studied the occurrence state of methane molecules in shales. Li et al. (2020) compared the immature shale samples in the extended formation of the Ordos Basin and mature shale samples in the Longmaxi Fm. They concluded that the shale gas first achieved saturated adsorption and partial dissolution with the increase in maturity before it was reserved in the pores as free gas. Finally, the dynamic balance was achieved between the adsorbed gas and free gas. The mentioned process corresponded with four occurrence evolution stages: adsorption, pores filling, fracture filling, and reservoir formation. Lv et al. (2020) carried out the physical experiment and mathematical model and studied the low-temperature liquid nitrogen adsorption experiment and scanning electron microscopy experiment. Pore characteristics and methane features of shales in the Longmaxi Fm. were studied based on the

molecular dynamics method. It was found that, with the increase in buried depth, the free gas content rocketed, outnumbering the adsorbed gas in the Longmaxi Fm. According to the methane adsorption features of shales in the Longmaxi Formation reservoir, with the changes in pore volume, the methane adsorption potential changed from positive to negative and ended up close to zero. The zero point means no methane molecules were adsorbed on the pore wall and that the occurrence state was mainly free instead of the adsorption state. As the shale gas has unequal adsorption mechanisms in different mineral pores, Xu et al. (2020) adopted Material Studio to simulate the occurrence state of shale gas in pore models of three minerals (kerogen, clay minerals, and quartz) and studied the adsorption mechanisms of shale gas in different mineral pores. The result showed that kerogen had the highest adsorption capacity, higher than that of clay minerals and then quartz. Moreover, the primary cause of massive variance in the adsorption capacity of organic matter, clay minerals, and clastic minerals lies in the adsorption sites' gas characteristics on the mineral surface.

In these years, massive exploration and advanced experiments on shale gas provided more data on the analysis of the adsorption state of methane in postmature marine shales with different agents. The research object in this study is the shales of the Lower Silurian Longmaxi Fm. of the upper Yangtze region in southern China. The SWY-1 well and the cores were selected for the total organic carbon (TOC) content analysis, organic matter maturity analysis, total gas content analysis, isothermal adsorption experiment, and scanning electron microscope observation. The ultimate aim is to clarify the occurrence of methane molecules in postmature marine shales (Figure 1).

GEOLOGICAL SETTINGS

Sedimentary and Stratum Characteristics

Based on previous studies, the upper Yangtze area was flanked by the Cathaysian Plate, forming an interior Cratonic sagging basin during the Late Ordovician–Early Silurian. The sedimentary strata formed in the Late Ordovician in the upper Yangtze area is referred to as Wefeng Fm., and that formed in the Early Silurian is called the Longmaxi Fm., which can be further divided into members 1, 2, and 3. The first member of the Longmaxi Fm., whose shales have different lithologies, was taken as the main study object. Specifically, the lower part of this member is primarily the black organic-rich siliceous shale, while dark gray shale, silty shale, and siltstone exist in the upper segment (Mei et al., 2012; Wang et al., 2015; Mou et al., 2019; Zhang et al., 2019a; Zhang et al., 2020b).

Tectonic Characteristics

According to previous research (Li et al., 1995; Li et al., 2002; Wang and Li, 2003; Zhang et al., 2017; Li et al., 2021), southern China has two plates of primary continental crust, i.e., the Yangtze Plate and Cathaysian Plate in the early Mesoproterozoic, which are in a state of tension during the Lower Cambrian when massive transgression took place.

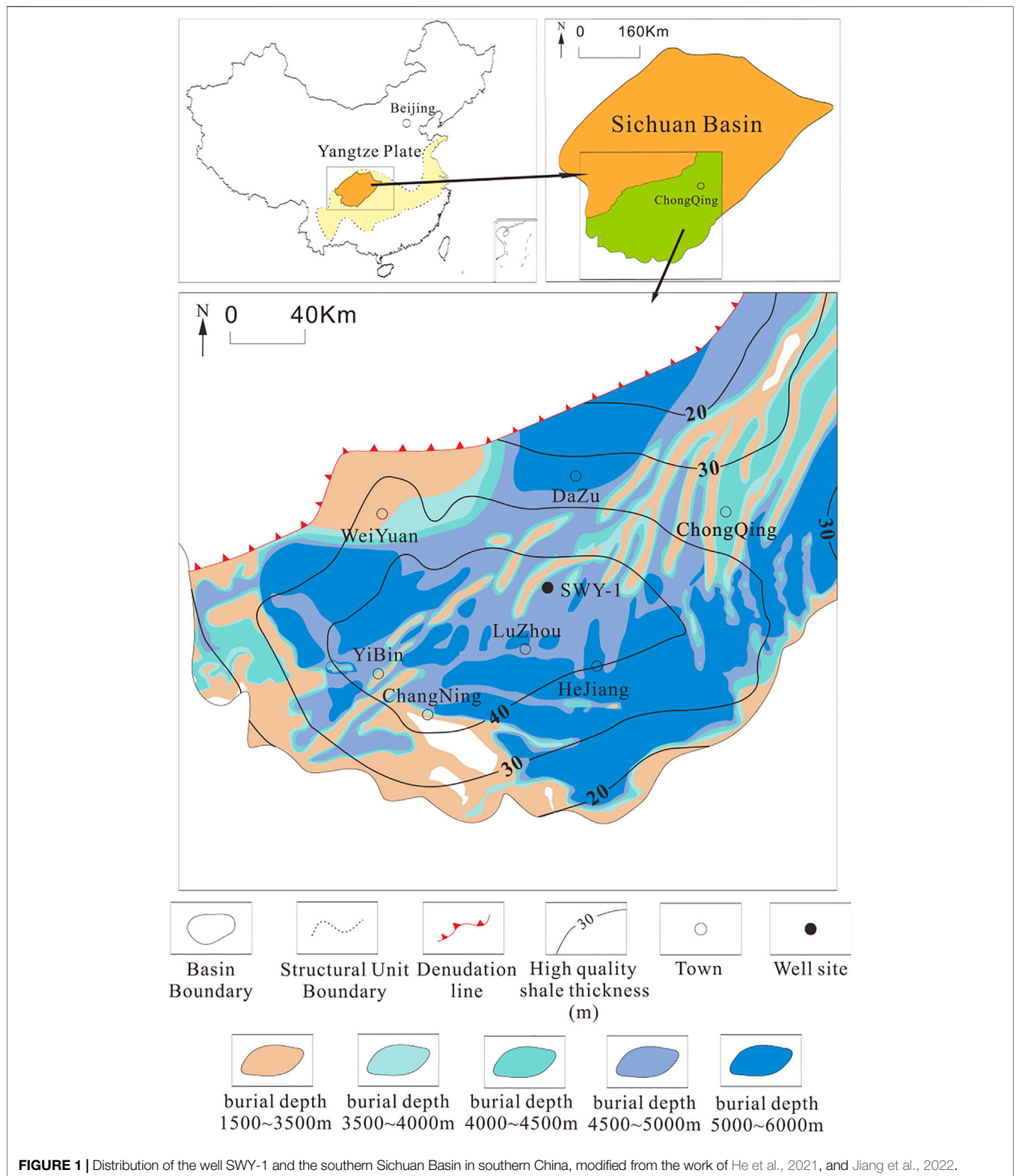


FIGURE 1 | Distribution of the well SWY-1 and the southern Sichuan Basin in southern China, modified from the work of He et al., 2021, and Jiang et al., 2022.

Consequently, a set of organic-rich shales covering almost the whole plate became sediment. Afterward, the water became shallow, and the lithology changed from fine shale and silty shale into coarse clastic rocks such as siltstone and sandstone.

During the Ordovician, the water body was shallower due to the extrusion and collision of the Cathaysian Plate, and the clastic rocks changed into carbonate rocks. The massive transgression reoccurred in the Upper Ordovician–Lower

TABLE 1 | Location and depth of core samples.

No.	Well	Fm.	Depth (m)	No.	Well	Fm.	Depth (m)
1	SWY-1	Longmaxi	4,024.29	7	SWY-1	Longmaxi	4085.46
2	SWY-1	Longmaxi	4,041.66	8	SWY-1	Longmaxi	4087.84
3	SWY-1	Longmaxi	4,053.95	9	SWY-1	Longmaxi	4089.63
4	SWY-1	Longmaxi	4,062.35	10	SWY-1	Longmaxi	4091.7
5	SWY-1	Longmaxi	4,072.92	11	SWY-1	Longmaxi	4092.91
6	SWY-1	Longmaxi	4,080.01	12	SWY-1	Longmaxi	4094.68

TABLE 2 | Analysis results of the mineral components of core samples.

Depth (m)	Quartz (%)	Potash feldspar (%)	Plagioclase (%)	Calcite (%)	Dolomite (%)	Pyrite (%)	Clay minerals (%)
4,024.29	31.5	0.7	7.6	0	0	3.2	57
4,041.66	33.3	0	6.2	0	0	2.7	57.8
4,053.95	35.9	0	7.1	2.9	6.4	5.1	42.6
4,062.35	29.9	0.9	3.6	5.5	12.4	3.7	44
4,072.92	42.1	0	8.4	2.5	5.2	3.1	38.7
4,080.01	44.3	0.9	6.9	3.5	3.4	4.7	36.3
4,085.46	57.5	0	3.4	6.9	9	2.6	20.6
4,087.84	64.4	1.1	3.3	3.7	4.7	3.8	19
4,089.63	42.2	0.9	4.4	4.5	9.7	7.3	31
4,091.7	51	0	1.4	4.2	21.9	3.6	17.9
4,092.91	31.7	1.1	5.1	2.9	5.7	3.8	49.7
4,094.68	18.4	1	3.8	0	2.8	8.2	65.8

TABLE 3 | Analysis results of the TOC contents and clay mineral components of core samples.

Depth (m)	TOC (%)	Clay minerals (%)	I/S mixed layer (%)	Illite (%)	Chlorite (%)
4,024.29	0.77	57	23.94	19.38	13.68
4,041.66	0.2	57.8	24.854	21.964	10.982
4,053.95	1.82	42.6	20.448	17.892	4.26
4,062.35	2.28	44	20.24	18.92	4.84
4,072.92	1.72	38.7	19.737	15.867	3.096
4,080.01	2.74	36.3	16.698	16.698	2.904
4,085.46	3.2	20.6	13.39	5.974	1.236
4,087.84	4.05	19	11.21	7.03	0.76
4,089.63	4.79	31	18.29	11.78	0.93
4,091.7	2.02	17.9	8.771	8.592	0.537
4,092.91	1.26	49.7	30.317	15.904	3.479
4,094.68	2.22	65.8	38.164	23.03	4.606

Silurian, restoring the sedimentary system of clastic rocks. Meanwhile, a set of sedimentary organic-rich shales were formed in the deep shelf surrounded by the ancient land. During the Cambrian–Silurian, the Cathaysian Plate gradually subducted down to and collided with the Yangtze Plate. Until the end of the Silurian, the Yangtze and Cathaysian Plates merged into a unified South China Plate.

SAMPLES, EXPERIMENTS, AND DATA SOURCES

Table 1 shows the depth of 12 core samples selected from the shales in the well SWY-1 of the Longmaxi Fm. In this study, the TOC content was measured using a Sievers 860 TOC

content analyzer, and the maturity of organic matter was analyzed by using a ZEISS Imager A2m, J&M MSP200 polarizing fluorescence microscope. In addition, the YST-I mineral analyzer was employed in X-ray mineral-wide and clay mineral analysis, and the 200812A shale gas content analyzer was used to test the gas content of cores in the well. An isothermal adsorption experiment was conducted using an HPVA-200-4 isothermal adsorption instrument at 110°C. FIB-SEM (focused ion beam-scanning electron microscopy) experiment was operated by using the Helios NanoLab 660, and FIB-HIM (focused ion beam-helium ion microscopy) was conducted by using the Zeiss Orion NanoFab. Some of the experimental data in this article came from the referred works (Guo et al., 2019; He et al., 2021; Jiang et al., 2022).

TABLE 4 | Analysis results of the Langmuir volume, Langmuir pressure, adsorbed gas, and total gas content of the core samples.

Depth (m)	Formation pressure (MPa)	Langmuir volume (m ³ /t)	Langmuir pressure (MPa)	Adsorbed gas content (m ³ /t)	Total gas content (m ³ /t)	Free gas content (m ³ /t)
4,024.29	39.48	1.07	3.84	0.98	1.37	0.39
4,041.66	39.65	0.31	0.37	0.31	1.51	1.20
4,053.95	39.77	1.22	0.51	1.20	2.58	1.38
4,062.35	39.85	1.58	2.36	1.49	2.37	0.88
4,072.92	39.96	0.73	0.39	0.72	2.34	1.62
4,080.01	40.02	1.88	2.99	1.75	3.69	1.94
4,085.46	40.08	1.28	0.54	1.26	4.93	3.67
4,087.84	40.10	1.41	0.7	1.39	5.67	4.28
4,089.63	40.12	1.72	1.19	1.67	6.23	4.56
4,091.7	40.14	1.25	2.2	1.19	4.66	3.47
4,092.91	40.15	0.5	1.09	0.49	3.03	2.54
4,094.68	40.17	0.77	0.97	0.75	4.84	4.09

RESULTS AND DISCUSSION

According to the test, the average maturity of organic matter in shales in the well SWY-1 of the Longmaxi Fm. was 2.1%, meaning the shale studied was the postmature marine shale. TOC content analysis, mineral component analysis, and isothermal adsorption experiment were conducted on the 12 shale core samples, and the results are shown in **Tables 2–4**. Langmuir volume refers to the maximum adsorbing capacity, whose physical denotation is the adsorbed gas content when the shales are saturated with methane at a given temperature, and the unit is m³/t. The Langmuir

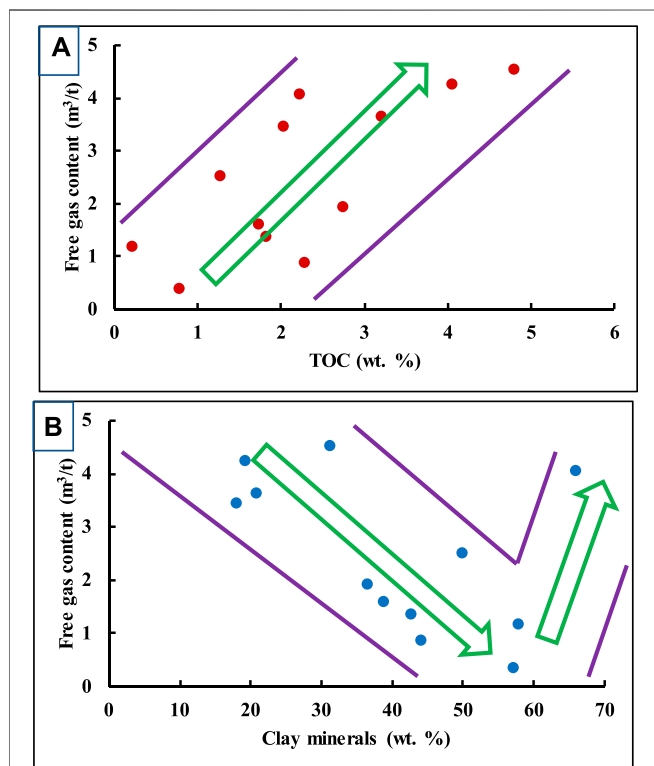


FIGURE 2 | Correlation analysis on the free gas content with the TOC content and clay mineral content. It can be seen that the free gas content is positively correlated with the TOC content, and it first negatively correlates and then positively correlates with clay minerals.

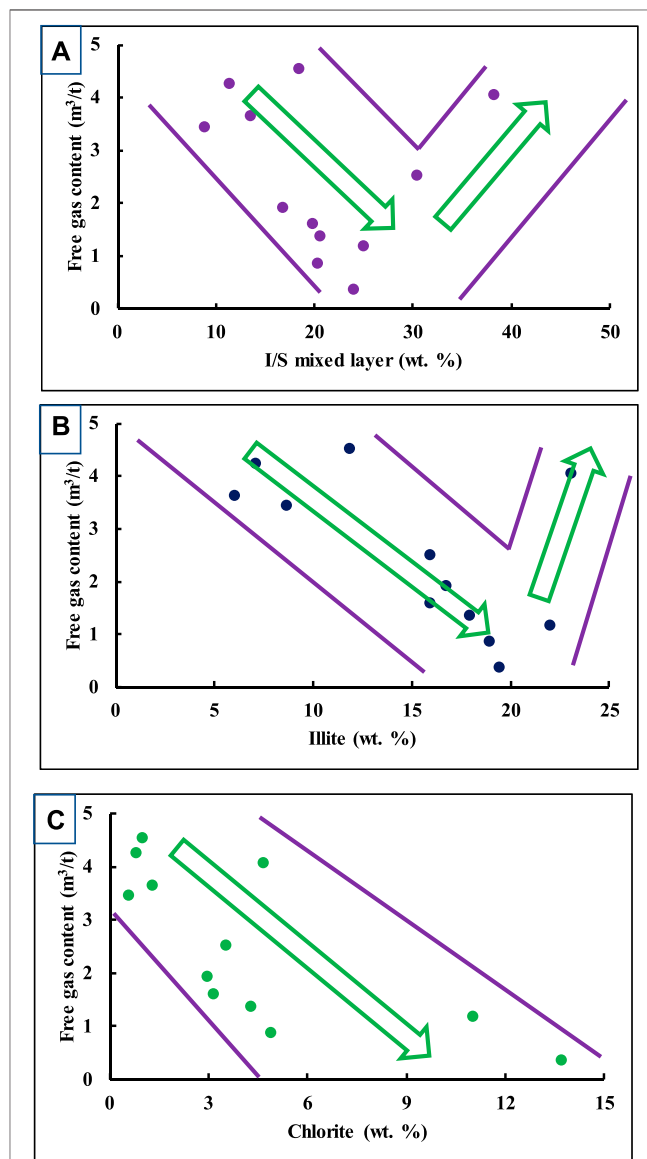
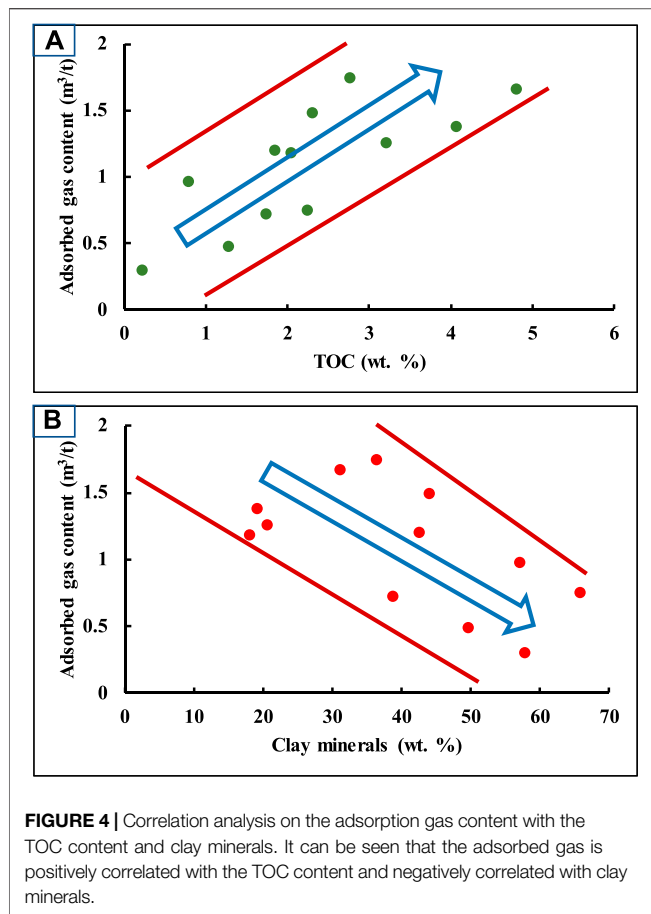


FIGURE 3 | Correlation analysis on the free gas content with the I/S mixed layer, illite, and chlorite. It could be seen that free gas is first negatively correlated and then positively correlated with the I/S mixed layer and illite content, while the free gas has negative relativity with chlorite.



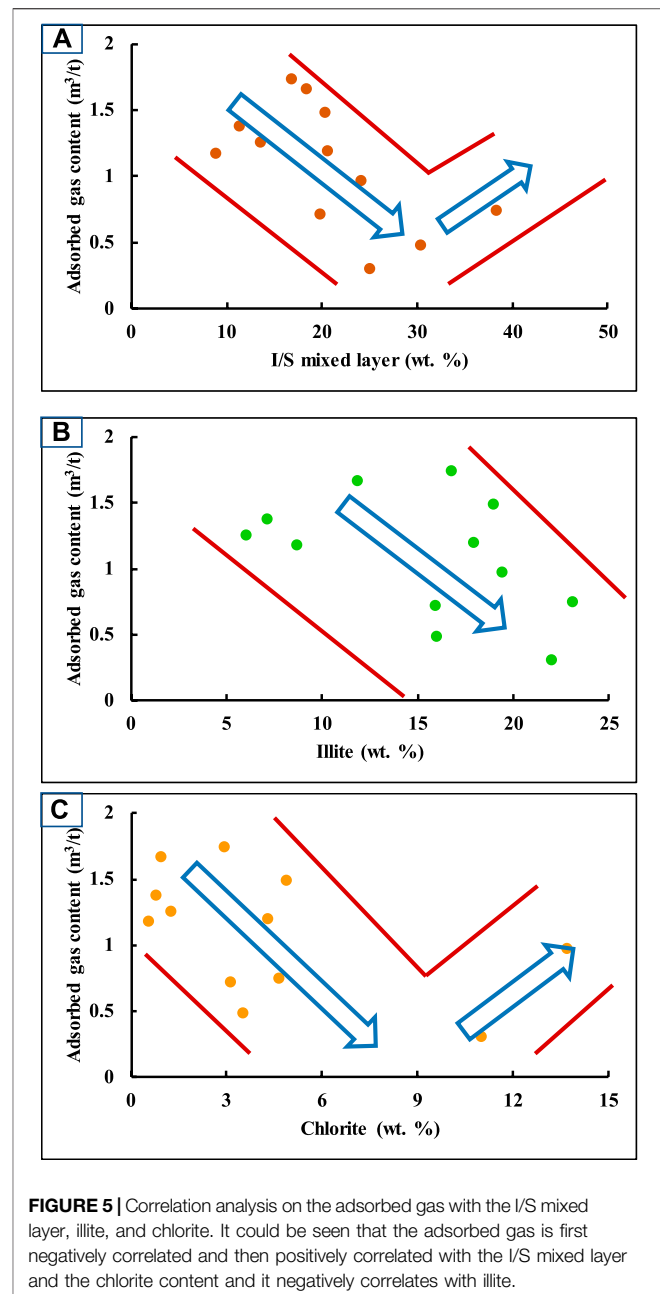
pressure means the corresponding pressure of half Langmuir in volume with the unit MPa (Chalmers and Bustin, 2008; Ji et al., 2014; Ji et al., 2015; Ji et al., 2016; Zhang et al., 2019b; Zhang et al., 2019c). Based on the following Langmuir equation, the shales' adsorption content of methane under any pressure can be calculated.

$$V = \frac{V_L P}{P + P_L},$$

where V refers to the adsorption content of the samples under formation pressure P , with m^3/t as the unit; P means the formation pressure, with MPa as the unit; $P = 1 \times 9.81 \times H / 1000$, where H is the depth, and its unit is m ; V_L refers to the volume of Langmuir; and P_L refers to the pressure of Langmuir.

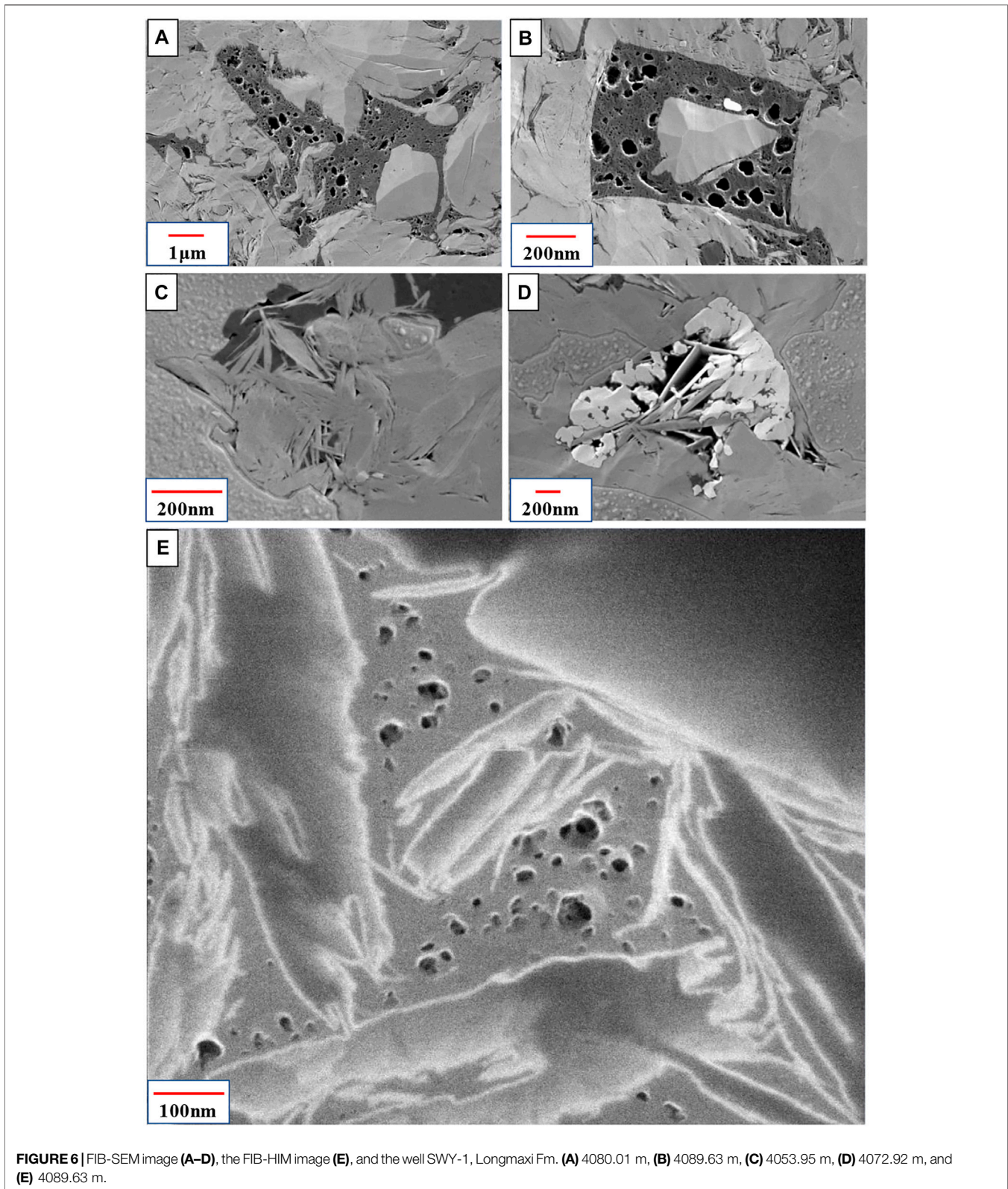
According to the depth and the equation mentioned earlier, the formation pressure can be calculated. The adsorption content of the shale can be achieved based on the Langmuir volume, pressure, and formation pressure. The adsorbed gas is subtracted from the total gas content in shales to get the free gas content, and the results are presented in **Table 4**.

This study conducted a correlation analysis on free gas content, adsorbed gas, TOC content, clay mineral content, I/S mixed layer, illite, and chlorite, respectively, and the results are presented in **Figures 2–5**. From **Figure 2**, it can be seen that the free gas content has positive relativity with the TOC content,



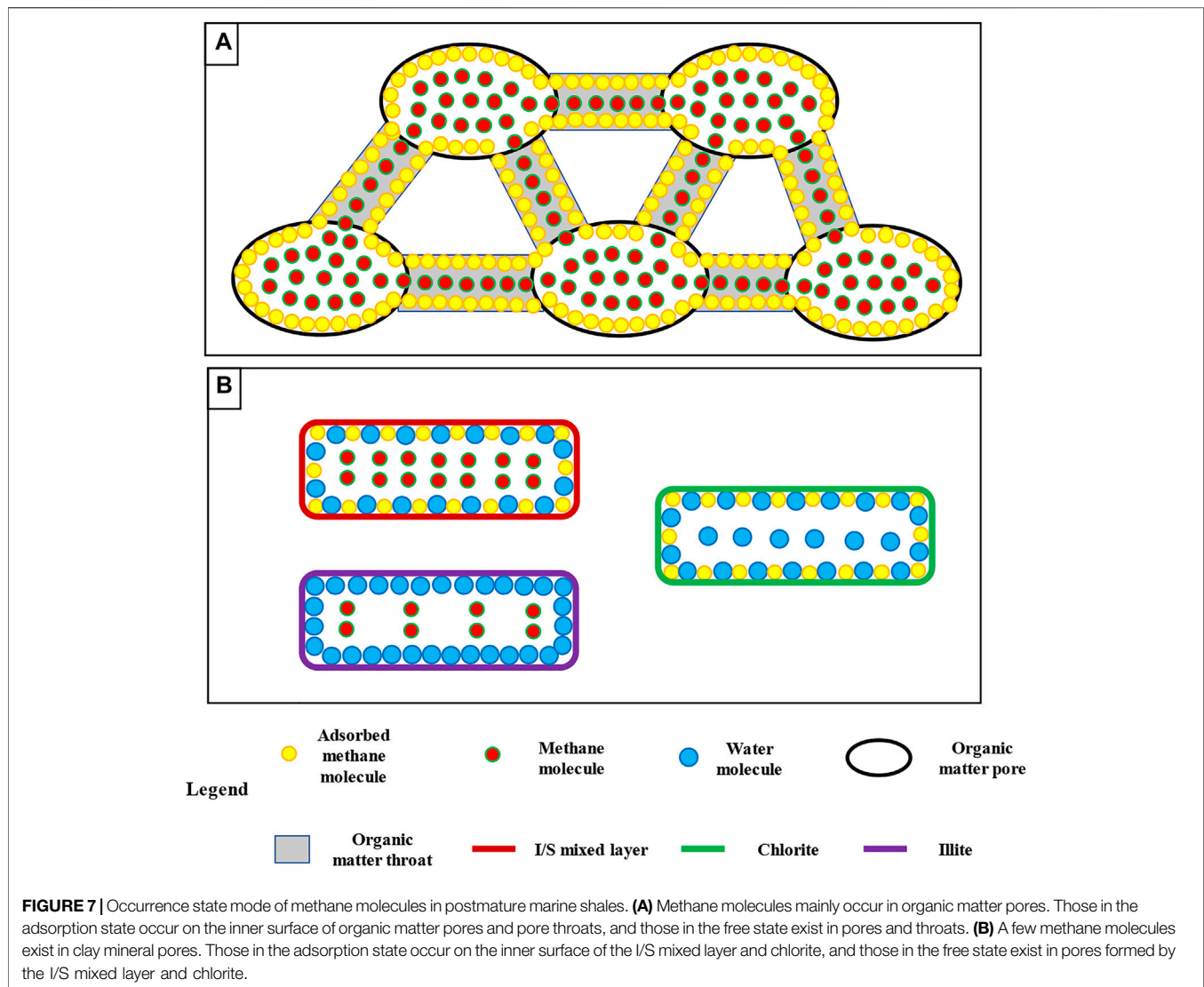
while it negatively correlates with the clay mineral content before they are positively correlated. With further analysis on the free gas content and clay mineral components, as shown in **Figure 3**, free gas is first negatively correlated and then positively correlated with the I/S mixed layer and illite content. Meanwhile, the free gas content has a negative relation with the chlorite content. These results show that the free gas mainly exists in the pores of the organic matter. Little can be found in the I/S mixed layer and illite and none in chlorite.

According to **Figure 4**, the adsorbed gas content is positively correlated with the TOC content and negatively correlated with clay mineral components. More analysis was conducted on the adsorbed gas content and mineral components. From **Figure 5**,



the adsorbed gas content is first negatively correlated and then positively correlated with the I/S mixed layer and chlorite. Meanwhile, it has a negative relation with the illite content.

These results show that the adsorbed gas mainly exists in the pores of organic matter. Little can be found in the I/S mixed layer and chlorite and none in illite.



The followings are the analyses of the causes. On the one hand, the strata water content primarily affects shales' capacity of storing methane because the water molecules occupy the reservoir space of free methane molecules and the adsorption sites of those in the adsorption state (Chen et al., 2017; Zhang et al., 2020a; Zhang et al., 2020c; Huang et al., 2020; Liu et al., 2021a; Liu et al., 2021b). As the strata shale reservoir usually contains water and the clay minerals have hydrophilicity, in underground reservoirs, the storage capacity of clay minerals tends to be inhibited. When there are enough clay minerals, the storage capacity will be presented (Chen et al., 2016; Zuo et al., 2019; Wang et al., 2020b; Zhang et al., 2022).

On the other hand, according to previous studies, some suppose that the adsorption sites are more intensive on the surface of organic matters, leading to better adsorption capacity. Gas molecules have a discrete distribution on the clay mineral surface and a relatively continuous distribution on the organic matter surface (Chen et al., 2018; Xia et al.,

2020; Gao, 2021; Guo et al., 2021; Shan et al., 2021). In addition, specific surface areas can influence the adsorption capacity to a large extent. Through comparison, it was found that the organic matter > I/S mixed layer > chlorite > illite in terms of the specific surface area of components in shales, which in organic matters outnumbers that in clay minerals.

The shale pore characteristics can be observed using a scanning electron microscope, from which it was seen that the FIB-SEM image has the largest grayscale, and the grayscale composed of different shale materials drops with the decrease in molecules. This means that the grayscale of the organic matter in the FIB-SEM image is higher than that of inorganic minerals (Tang et al., 2016; Wang et al., 2016a; Wang et al., 2016b; Wang et al., 2017). According to the FIB-SEM image in **Figures 6A,B**, tremendous organic matter pores exist in shales with relatively high roundness. The FIB-SEM image in **Figures 6C,D** shows clay mineral pores in shales, triangles, and flakes in shape with low roundness (Li et al., 2017a; Li et al., 2017b; Wang et al., 2020c).

The FIB-HIM image can reflect interior pore situations, presenting a 3D effect of the two-dimensional image. Different from the FIB-SEM image, the grayscale in FIB-HIM increases with the decrease in molecules, which means its organic matter grayscale is lower than inorganic minerals. From **Figure 6E**, it can be seen that many tiny pores are embedded in the large organic matter pores, resulting in high connectivity and an alveolate structure.

Based on the earlier analysis, this study summarized the occurrence state of methane in postmature marine shales. As shown in **Figure 7A**, the organic matter pore is approximately round. The pores are large in amount with excellent connectivity. The huge space between pores and inside the pore throat can store abundant free gas. The inner surface of the organic matter pore and throat adsorb methane molecules densely and successively (Li et al., 2018; Wang et al., 2020d; Hou et al., 2020; Xiao et al., 2020). The large pore-specific surface area of organic matter offers methane molecules with more adsorption spaces.

As shown in **Figure 7B**, the clay mineral pores are flaky in shape. Thus, they are prone to contain water compared with organic matter pores. With a smaller pore-specific surface area, the clay minerals have a loose surface, so the adsorption of methane proceeds with interruptions. Among the three clay minerals in postmature marine shales in the Longmaxi Fm., the I/S mixed layer has the largest mineral layer spacing with powerful adsorption capacity, offering reservoir spaces for free gas and adsorbed methane molecules. Chlorite has average adsorption capacity, but due to its small mineral layer spacing, it only stores a little adsorbed gas and rare free gas. As for illite, it has poor methane adsorption capacity with certain mineral layer spacing. Thus, adsorbed gas can hardly be stored, and only a small amount of free gas could be gathered in illite.

CONCLUSION

In this study, the cores selected from the shales of the Lower Silurian Longmaxi Fm. of the upper Yangtze region in southern China were taken as study objects. The analyses of TOC content, organic matter maturity, and mineral components and experiments on core gas content, isothermal adsorption, FIB-SEM, and FIB-HIM were conducted. The following results were obtained based on analyzing the occurrence state of methane molecules in postmature marine shales with different agents.

First, the majority of methane molecules exist in organic matter pores of postmature marine shales. These pores are large in number with high roundness in the organic-rich shales with the organic matter. The connectivity is excellent, presenting a structure of small pores embedded in big ones. Huge spaces are observed in pores and throats, allowing the storage of tremendous free gas. In addition, the pore-specific surface area of organic matter pores and throats

is larger. Inside, the methane molecules can be adsorbed densely and continuously, offering more spaces for adsorbing methane molecules.

Second, a few methane molecules exist in the clay mineral pores of postmature marine shales. The clay minerals are flaky in shape with a small number of pores with low roundness. Compared with the organic matter pores, the pore-specific surface area of clay minerals is smaller, so the adsorption of methane molecules is not smooth. There are three clay minerals in postmature marine shales in the Longmaxi Fm. The I/S mixed layer has a large mineral layer gap and strong adsorbing capacity, offering reservoir spaces. Chlorite can adsorb methane molecules, but the mineral layer gap is small. Thus, it stores a little adsorbed gas but cannot store free gas. By contrast, illite has comparably poor adsorption capacity, but it has certain mineral layer spacing, so the adsorbed gas cannot be stored. However, it can store certain free gas.

DATA AVAILABILITY STATEMENT

The raw data supporting the conclusion of this article will be made available by the authors, without undue reservation.

AUTHOR CONTRIBUTIONS

KZ, YS, and ZJ contributed to the conception and design of the study. KZ organized the database. YS performed the statistical analysis. KZ, YS, and ZJ wrote the first draft of the manuscript. XY, XW, FH, LZ, LT, PL, YY, YZ, XC, and ZZ wrote the sections of the manuscript. All authors contributed to manuscript revision, read, and approved the submitted version.

FUNDING

This study was supported by the National Natural Science Foundation of China (Nos. 42102192, 42130803, and 42072174), the open experiment fund of Southwest Petroleum University (2021KSP02029), the open fund of the Key Laboratory of Tectonics and Petroleum Resources (China University of Geosciences), the Ministry of Education, Wuhan (TPR-2020-07), the open fund from the State Key Laboratory of Petroleum Resources and Prospecting (PRP/open-2107), the open fund from the State Key Laboratory of Shale Oil and Gas Enrichment Mechanisms and Effective Development (G5800-20-ZS-KFGY012), and the Science and Technology Cooperation Project of the CNPC-SWPU Innovation Alliance.

ACKNOWLEDGMENTS

We sincerely appreciate all reviewers and the handling editor for their critical comments and constructive suggestions.

REFERENCES

- Avraam, C., Chu, D., and Siddiqui, S. (2020). Natural Gas Infrastructure Development in North America under Integrated Markets. *Energy Policy* 147, 111757. doi:10.1016/j.enpol.2020.111757
- Chalmers, G. R. L., and Bustin, R. M. M. (2008). Lower Cretaceous Gas Shales in Northeastern British Columbia, Part II: Evaluation of Regional Potential Gas Resources. *Bull. Can. Pet. Geology*. 56 (1), 22–61. doi:10.2113/gscpgbull.56.1.22
- Chen, G., Lu, S., Zhang, J., Xue, Q., Han, T., Xue, H., et al. (2016). Research of CO₂ and N₂ Adsorption Behavior in K-illite Slit Pores by GCMC Method. *Sci. Rep.* 6 (1), 1–10. doi:10.1038/srep37579
- Chen, G., Lu, S., Li, J., Xue, H., Wang, M., Tian, S., et al. (2017). A Method to Recover the Original Total Organic Carbon Content and Cracking Potential of Source Rocks Accurately Based on the Hydrocarbon Generation Kinetics Theory. *J. Nanosci. Nanotechnol.* 17 (9), 6169–6177. doi:10.1166/jnn.2017.14407
- Chen, G., Lu, S., Liu, K., Han, T., Xu, C., Xue, Q., et al. (2018). GCMC Simulations on the Adsorption Mechanisms of CH₄ and CO₂ in K-illite and Their Implications for Shale Gas Exploration and Development. *Fuel* 224, 521–528. doi:10.1016/j.fuel.2018.03.061
- Chen, G., Lu, S., Liu, K., Xue, Q., Han, T., Xu, C., et al. (2019). Critical Factors Controlling Shale Gas Adsorption Mechanisms on Different Minerals Investigated Using GCMC Simulations. *Mar. Pet. Geology*. 100, 31–42. doi:10.1016/j.marpetgeo.2018.10.023
- Dong, D., Shi, Z., Guan, Q., Jiang, S., Zhang, M., Zhang, C., et al. (2018). Progress, Challenges and Prospects of Shale Gas Exploration in the Wufeng-Longmaxi Reservoirs in the Sichuan Basin. *Nat. Gas Industry B* 5 (5), 415–424. doi:10.1016/j.ngib.2018.04.011
- Gao, F. (2021). Influence of Hydraulic Fracturing of strong Roof on Mining-Induced Stress Insight from Numerical Simulation. *J. Mining Strata Control. Eng.* 3 (2), 023032. doi:10.13532/j.jmsce.cn10-1638/td.20210329.001
- Gao, Z., Fan, Y., Xuan, Q., and Zheng, G. (2020). A Review of Shale Pore Structure Evolution Characteristics with Increasing thermal Maturities. *Adv. Geo-energy Res.* 4 (3), 247–259. doi:10.46690/ager.2020.03.03
- Guo, X., Hu, D., Liu, R., Wei, X., and Wei, F. (2019). Geological Conditions and Exploration Potential of Permian marine-continent Transitional Facies Shale Gas in the Sichuan Basin. *Nat. Gas Industry B* 6 (3), 198–204. doi:10.1016/j.ngib.2018.10.002
- Guo, H., Ji, M., Sun, Z., and Zhou, Z. (2021). Energy Evolution Characteristics of Red sandstone under Cyclic Load. *J. Mining Strata Control. Eng.* 3 (4), 043019. doi:10.13532/j.jmsce.cn10-1638/td.20211008.001
- He, Z., Nie, H., and Jiang, T. (2021). Challenges and Countermeasures of Effective Development with Large Scale of Deep Shale Gas in Sichuan Basin. *Reservoir Eval. Dev.* 11, 1–11. (in Chinese with English abstract). doi:10.13809/j.cnki.cn32-1825/te.2021.02.001
- Hou, E., Cong, T., Xie, X., and Wei, J. (2020). Ground Surface Fracture Development Characteristics of Shallow Double Coal Seam Staggered Mining Based on Particle Flow. *J. Mining Strata Control. Eng.* 2 (1), 013521. doi:10.13532/j.jmsce.cn10-1638/td.2020.01.002
- Huang, H., Li, R., Jiang, Z., Li, J., and Chen, L. (2020). Investigation of Variation in Shale Gas Adsorption Capacity with Burial Depth: Insights from the Adsorption Potential Theory. *J. Nat. Gas Sci. Eng.* 73, 103043. doi:10.1016/j.jngse.2019.103043
- Huang, X., and Zhao, Y.-P. (2017). Characterization of Pore Structure, Gas Adsorption, and Spontaneous Imbibition in Shale Gas Reservoirs. *J. Pet. Sci. Eng.* 159, 197–204. doi:10.1016/j.petrol.2017.09.010
- Ji, W., Song, Y., Jiang, Z., Wang, X., Bai, Y., and Xing, J. (2014). Geological Controls and Estimation Algorithms of Lacustrine Shale Gas Adsorption Capacity: a Case Study of the Triassic Strata in the Southeastern Ordos Basin China. *Int. J. Coal Geology*. 134–135, 61–73. doi:10.1016/j.coal.2014.09.005
- Ji, W., Song, Y., Jiang, Z., Chen, L., Li, Z., Yang, X., et al. (2015). Estimation of marine Shale Methane Adsorption Capacity Based on Experimental Investigations of Lower Silurian Longmaxi Formation in the Upper Yangtze Platform, south China. *Mar. Pet. Geology*. 68, 94–106. doi:10.1016/j.marpetgeo.2015.08.012
- Ji, W., Song, Y., Jiang, Z., Meng, M., Liu, Q., Chen, L., et al. (2016). Fractal Characteristics of Nano-Pores in the Lower Silurian Longmaxi Shales from the Upper Yangtze Platform, south China. *Mar. Pet. Geology*. 78, 88–98. doi:10.1016/j.marpetgeo.2016.08.023
- Jiang, L., Song, Y., Liu, W., Chen, Z., Zhang, H., and He, F. (2022). Study on the State of Methane Molecule Adsorption on Different media in Highly Evolved marine Shales--A Case Study on the Shales from the Lower Silurian Longmaxi Formation in the Sichuan Basin, Southern China. *Front. Earth Sci.* 9, 1333. doi:10.3389/feart.2021.829653
- Kang, H., Xu, G., Wang, B., Wu, Y., Jiang, P., Pan, J., et al. (2019). Forty Years Development and Prospects of Underground Coal Mining and Strata Control Technologies in China. *J. Mining Strata Control. Eng.* 1 (1), 013501. doi:10.13532/j.jmsce.cn10-1638/td.2019.02.002
- Li, Z.-X., Zhang, L., and Powell C, M. (1995). South China in Rodinia: Part of the Missing Link between Australia-east Antarctica and Laurentia. *Geology* 23 (5), 407–410. doi:10.1130/0091-7613(1995)023<0407:scirpo>2.3.co;2
- Li, Z.-X., Li, X.-h., Zhou, H., and Kinny, P. D. (2002). Grenvillian continental Collision in South China: New SHRIMP U-Pb Zircon Results and Implications for the Configuration of Rodinia. *Geol.* 30 (2), 163–166. doi:10.1130/0091-7613(2002)030<0163:gccisc>2.0.co;2
- Li, T., Jiang, Z., Li, Z., Wang, P., Xu, C., Liu, G., et al. (2017a). Continental Shale Pore Structure Characteristics and Their Controlling Factors: A Case Study from the Lower Third Member of the Shahejie Formation, Zhanhua Sag, Eastern China. *J. Nat. Gas Sci. Eng.* 45, 670–692. doi:10.1016/j.jngse.2017.06.005
- Li, T., Jiang, Z., Xu, C., Liu, B., Liu, G., Wang, P., et al. (2017b). Effect of Pore Structure on Shale Oil Accumulation in the Lower Third Member of the Shahejie Formation, Zhanhua Sag, Eastern China: Evidence from Gas Adsorption and Nuclear Magnetic Resonance. *Mar. Pet. Geology*. 88, 932–949. doi:10.1016/j.marpetgeo.2017.09.030
- Li, X., Jiang, Z., Wang, P., Song, Y., Li, Z., Tang, X., et al. (2018). Porosity-preserving Mechanisms of marine Shale in Lower Cambrian of Sichuan Basin, South China. *J. Nat. Gas Sci. Eng.* 55, 191–205. doi:10.1016/j.jngse.2018.05.002
- Li, Q., Tang, L., and Pang, X. (2020). Dynamic Evolution Model of Shale Gas Occurrence and Quantitative Evaluation of Gas-Bearing Capacity. *Geol. Rev.* 66 (2), 457–466. (in Chinese with English abstract). doi:10.16509/j.georeview.2020.02.014
- Li, X., Jiang, Z., Jiang, S., Wang, S., Miao, Y., Wu, F., et al. (2021). Synergetic Effects of Matrix Components and Diagenetic Processes on Pore Properties in the Lower Cambrian Shale in Sichuan Basin, South China. *J. Nat. Gas Sci. Eng.* 94, 104072. doi:10.1016/j.jngse.2021.104072
- Liu, B., He, S., Meng, L., Fu, X., Gong, L., and Wang, H. (2021a). Sealing Mechanisms in Volcanic Faulted Reservoirs in Xujiaweizi Extension Northern Songliao Basin Northeastern China. *AAPG Bull.* 105, 1721–1743. doi:10.1306/03122119048
- Liu, B., Sun, J., Zhang, Y., He, J., Fu, X., Yang, L., et al. (2021b). Reservoir Space and Enrichment Model of Shale Oil in the First Member of Cretaceous Qingshankou Formation in the Changling Sag, Southern Songliao Basin, NE China. *Pet. Exploration Dev.* 48 (3), 608–624. doi:10.1016/s1876-3804(21)60049-6
- Lv, Z., Tian, Y., Su, J., Liu, N., and Ji, W. (2020). Pore Characteristics and Occurrence Characteristics of marine Organic-Rich Shale in Sichuan Basin. *Sci. Tech. Eng.* 20 (33), 13568–13574. (in Chinese with English abstract). doi:10.3969/j.issn.1671-1815.2020.33.008
- Ma, X. (2019). Enrichment Laws and Scale Effective Development of Shale Gas in the Southern Sichuan Basin. *Nat. Gas Industry B* 6 (3), 240–249. doi:10.1016/j.ngib.2018.10.005
- Mei, L., Deng, D., Shen, C., and Liu, S. (2012). Tectonic Dynamics and marine Hydrocarbon Accumulation of Jiangnan-Xuefeng Uplift. *Geol. Sci. Tech. Inf.* 31 (5), 85–93. (in Chinese with English abstract).
- Mou, C., Wang, X., Wang, Q., Zhou, K., Liang, W., Ge, X., et al. (2019). Relationship between Sedimentary Facies and Shale Gas Geological Conditions of the Lower Silurian Longmaxi Formation in Southern Sichuan Basin and its Adjacent Areas. *J. Palaeogeogr.* 18 (3), 457–472. (in Chinese with English abstract). doi:10.7605/gdxb.2016.03.032
- Shan, S., Wu, Y., Fu, Y., and Zhou, P. (2021). Shear Mechanical Properties of Anchored Rock Mass under Impact Load. *J. Mining Strata Control. Eng.* 3 (4), 043034. doi:10.13532/j.jmsce.cn10-1638/td.20211014.001
- Shang Xu, S., Gou, Q., Hao, F., Zhang, B., Shu, Z., Lu, Y., et al. (2020). Shale Pore Structure Characteristics of the High and Low Productivity wells, Jiaoshiba Shale Gas Field, Sichuan Basin, China: Dominated by Lithofacies or Preservation Condition. *Mar. Pet. Geology*. 114, 104211. doi:10.1016/j.marpetgeo.2019.104211

- Swiech, E., Wandycz, P., Eisner, L., Pasternacki, A., and Mackowski, T. (2017). Downhole Microseismic Monitoring of Shale Deposits Case Study from Northern Poland. *Acta Geodynamica et Geomaterialia* 14, 297–304. doi:10.13168/agg.2017.0012
- Tang, X., Jiang, Z., Jiang, S., Wang, P., and Xiang, C. (2016). Effect of Organic Matter and Maturity on Pore Size Distribution and Gas Storage Capacity in High-Mature to post-mature Shales. *Energy Fuels* 30 (11), 8985–8996. doi:10.1021/acs.energyfuels.6b01499
- Wang, J., and Li, Z. (2003). History of Neoproterozoic Rift Basins in South China: Implications for Rodinia Break-Up. *Precambrian Res.* 122 (1/4), 141–158. doi:10.1016/s0301-9268(02)00209-7
- Wang, J. (2019). Sustainable Coal Mining Based on Mining Ground Control. *J. Mining Strata Control. Eng.* 1 (1), 013505. doi:10.13532/j.jmsce.cn10-1638/td.2019.02.003
- Wang, Y., Dong, D., Li, X., Huang, J., Wang, S., and Wu, W. (2015). Stratigraphic Sequence and Sedimentary Characteristics of Lower Silurian Longmaxi Formation in the Sichuan Basin and its Peripheral Areas. *Nat. Gas Industry* 35 (3), 12–21. (in Chinese with English abstract). doi:10.1016/j.ngib.2015.07.014
- Wang, P., Jiang, Z., Chen, L., Yin, L., Li, Z., Zhang, C., et al. (2016a). Pore Structure Characterization for the Longmaxi and Niutitang Shales in the Upper Yangtze Platform, South China: Evidence from Focused Ion Beam-He Ion Microscopy, Nano-Computerized Tomography and Gas Adsorption Analysis. *Mar. Pet. Geology* 77, 1323–1337. doi:10.1016/j.marpetgeo.2016.09.001
- Wang, P., Jiang, Z., Ji, W., Zhang, C., Yuan, Y., Chen, L., et al. (2016b). Heterogeneity of Intergranular, Intraparticle and Organic Pores in Longmaxi Shale in Sichuan Basin, South China: Evidence from SEM Digital Images and Fractal and Multifractal Geometries. *Mar. Pet. Geology* 72, 122–138. doi:10.1016/j.marpetgeo.2016.01.020
- Wang, P., Jiang, Z., Yin, L., Chen, L., Li, Z., Zhang, C., et al. (2017). Lithofacies Classification and its Effect on Pore Structure of the Cambrian marine Shale in the Upper Yangtze Platform, South China: Evidence from FE-SEM and Gas Adsorption Analysis. *J. Pet. Sci. Eng.* 156, 307–321. doi:10.1016/j.petrol.2017.06.011
- Wang, G., Pang, Y., and Ren, H. (2020a). Intelligent Coal Mining Pattern and Technological Path. *J. Mining Strata Control. Eng.* 2 (1), 013501. doi:10.13532/j.jmsce.cn10-1638/td.2020.01.001
- Wang, J., Zhang, C., Zheng, D., Song, W., and Ji, X. (2020b). Stability Analysis of Roof in Goaf Considering Time Effect. *J. Mining Strata Control. Eng.* 2 (1), 013011. doi:10.13532/j.jmsce.cn10-1638/td.2020.01.005
- Wang, P., Yao, S., Jin, C., Li, X., Zhang, K., Liu, G., et al. (2020c). Key Reservoir Parameter for Effective Exploration and Development of High-Over Matured marine Shales: A Case Study from the Cambrian Niutitang Formation and the Silurian Longmaxi Formation, south China. *Mar. Pet. Geology* 121, 104619. doi:10.1016/j.marpetgeo.2020.104619
- Wang, P., Zhang, C., Li, X., Zhang, K., Yuan, Y., Zang, X., et al. (2020d). Organic Matter Pores Structure and Evolution in Shales Based on the He Ion Microscopy (HIM): A Case Study from the Triassic Yanchang, Lower Silurian Longmaxi and Lower Cambrian Niutitang Shales in China. *J. Nat. Gas Sci. Eng.* 84, 103682. doi:10.1016/j.jngse.2020.103682
- Wei, Y.-M., Kang, J.-N., Yu, B.-Y., Liao, H., and Du, Y.-F. (2017). A Dynamic Forward-Citation Full Path Model for Technology Monitoring: An Empirical Study from Shale Gas Industry. *Appl. Energ.* 205, 769–780. doi:10.1016/j.apenergy.2017.08.121
- Xia, Y., Lu, C., Yang, G., Su, S., Pang, L., Ding, G., et al. (2020). Experimental Study on Axial Fracture Cutting and Fracturing of Abrasive Jet in Hard Roof Hole. *J. Mining Strata Control. Eng.* 2 (3), 033522. doi:10.13532/j.jmsce.cn10-1638/td.20200522.001
- Xiao, J., Hao, Q., Zhang, S., and Fan, S. (2020). Influence of Oil Well Casing on the Law of Strata Pressure in Working Face. *J. Mining Strata Control. Eng.* 2 (1), 013522. doi:10.13532/j.jmsce.cn10-1638/td.2020.01.003
- Xu, C., Xue, H., Li, B., Lu, S., Zhang, J., Chen, G., et al. (2020). Microscopic Adsorption Mechanism Difference in the Mineral Pore of Shale Gas Reservoir. *Spec. oil gas reservoirs* 27 (4), 79–84. (in Chinese with English abstract). doi:10.3969/j.issn.1006-6535.2020.04.012
- Yu, X., Bian, J., and Liu, C. (2022). Determination of energy release parameters of hydraulic fracturing roof near goaf based on surrounding rock control of dynamic pressure roadway. *Journal of Mining and Strata Control. Engineering* 4 (1), 013016. doi:10.13532/j.jmsce.cn10-1638/td.20210908.001
- Zhang, K., Jiang, Z., Yin, L., Gao, Z., Wang, P., Song, Y., et al. (2017). Controlling Functions of Hydrothermal Activity to Shale Gas Content-Taking Lower Cambrian in Xiuwu Basin as an Example. *Mar. Pet. Geology* 85, 177–193. doi:10.1016/j.marpetgeo.2017.05.012
- Zhang, K., Song, Y., Jia, C., Jiang, Z., Jiang, S., Huang, Y., et al. (2019a). Vertical Sealing Mechanism of Shale and its Roof and Floor and Effect on Shale Gas Accumulation, a Case Study of marine Shale in Sichuan basin, the Upper Yangtze Area. *J. Pet. Sci. Eng.* 175, 743–754. doi:10.1016/j.petrol.2019.01.009
- Zhang, K., Song, Y., Jiang, S., Jiang, Z., Jia, C., Huang, Y., et al. (2019c). Shale Gas Accumulation Mechanism in a Syncline Setting Based on Multiple Geological Factors: An Example of Southern Sichuan and the Xiuwu Basin in the Yangtze Region. *Fuel* 241, 468–476. doi:10.1016/j.fuel.2018.12.060
- Zhang, K., Song, Y., Jiang, S., Jiang, Z., Jia, C., Huang, Y., et al. (2019b). Mechanism Analysis of Organic Matter Enrichment in Different Sedimentary Backgrounds: A Case Study of the Lower Cambrian and the Upper Ordovician-Lower Silurian, in Yangtze Region. *Mar. Pet. Geology* 99, 488–497. doi:10.1016/j.marpetgeo.2018.10.044
- Zhang, N., Han, C., and Xie, Z. (2019d). Theory of Continuous Beam Control and High Efficiency Supporting Technology in Coal Roadway. *J. Mining Strata Control. Eng.* 1 (1), 013005. doi:10.13532/j.jmsce.cn10-1638/td.2019.02.004
- Zhang, K., Jia, C., Song, Y., Jiang, S., Jiang, Z., Wen, M., et al. (2020a). Analysis of Lower Cambrian Shale Gas Composition, Source and Accumulation Pattern in Different Tectonic Backgrounds: A Case Study of Weiyuan Block in the Upper Yangtze Region and Xiuwu Basin in the Lower Yangtze Region. *Fuel* 263, 115978. doi:10.1016/j.fuel.2019.115978
- Zhang, K., Peng, J., Liu, W., Li, B., Xia, Q., Cheng, S., et al. (2020b). The role of deep geofluids in the enrichment of sedimentary organic matter: a case study of the Late Ordovician-Early Silurian in the upper Yangtze region and early Cambrian in the lower Yangtze region south China. *Geofluids* 2020, 8868638. doi:10.1155/2020/8868638
- Zhang, K., Peng, J., Wang, X., Jiang, Z., Song, Y., Jiang, L., et al. (2020c). Effect of Organic Maturity on Shale Gas Genesis and Pores Development: A Case Study on marine Shale in the Upper Yangtze Region, South China. *Open Geosciences* 12, 1617–1629. doi:10.1515/geo-2020-0216
- Zhang, K., Jiang, S., Zhao, R., Wang, P., Jia, C., and Song, Y. (2022). Connectivity of organic matter pores in the Lower Silurian Longmaxi Formation shale, Sichuan Basin, Southern China: Analyses from helium ion microscope and focused ion beam scanning electron microscope. *Geological Journal*, 1–13. doi:10.1002/gj.4387
- Zuo, J., Yu, M., Hu, S., Song, H., Wei, X., Shi, Y., et al. (2019). Experimental Investigation on Fracture Mode of Different Thick Rock Strata. *J. Mining Strata Control. Eng.* 1 (1), 013007. doi:10.13532/j.jmsce.cn10-1638/td.2019.02.008

Conflict of Interest: The authors declare that the research was conducted in the absence of any commercial or financial relationships that could be construed as a potential conflict of interest.

Publisher's Note: All claims expressed in this article are solely those of the authors and do not necessarily represent those of their affiliated organizations, or those of the publisher, the editors, and the reviewers. Any product that may be evaluated in this article, or claim that may be made by its manufacturer, is not guaranteed or endorsed by the publisher.

Copyright © 2022 Zhang, Song, Jiang, Yuan, Wang, Han, Zhang, Tang, Liu, Yang, Zeng, Chen and Zheng. This is an open-access article distributed under the terms of the Creative Commons Attribution License (CC BY). The use, distribution or reproduction in other forums is permitted, provided the original author(s) and the copyright owner(s) are credited and that the original publication in this journal is cited, in accordance with accepted academic practice. No use, distribution or reproduction is permitted which does not comply with these terms.